Fast all-focus image reconstruction method based on light field imaging

Shuzhen Wang[1], *Haili* Zhao[1,*], and *Wenbo* Jing[2]

[1]School of Electronic Information and Engineering, Changchun University of Science and Technology, Changchun, Jilin 130022, China
[2]School of Opto-Electronic Engineering, Changchun University of Science and Technology, Changchun, Jilin 130022, China

Abstract. To achieve high-quality imaging of all focal planes with large depth of field information, a fast all-focus image reconstruction technology based on light field imaging is proposed: combining light field imaging to collect field of view information, and using light field reconstruction to obtain a multi-focus image source set, using the improved NSML image fusion method performs image fusion to quickly obtain an all-focus image with a large depth of field. Experiments have proved that this method greatly reduces the time consumed in the image fusion process by simplifying the calculation process of NSML, and improves the efficiency of image fusion. This method not only achieves excellent fusion image quality, but also improves the real-time performance of the algorithm.

1 Introduction

The light field camera can calculate a refocused image at any depth in space after a single shot, which is the most prominent technical highlight of the light field camera that has received general attention [1, 2]. Based on this, the acquisition of high-quality texture images of various light fields and the calculation of high-precision depth information have been deeply studied[3]. Because it is not limited by the multiple focus shooting of traditional cameras to obtain multi-focus images, all-focus image fusion based on light field digital refocusing technology has become an important branch application of light field cameras[4].

At present, all-focus fusion for traditional images is mainly divided into spatial domain[5, 6] and transform domain[7-9]. The spatial domain performs definition evaluation based on pixels or blocks, and extracts high-quality pixels from different images to form a full-focus image. The calculation time is fast but there is a problem of blocking effects. The transform domain decomposes the image into sub-images of different resolution layers or different frequency bands. By evaluating the reconstruction of the resolution layer or sub-images to construct a refocused image, the blocking effect can be effectively avoided[10]. The currently commonly used focus evaluation functions in the spatial domain mainly include the Spatial Frequency method (SF), the Energy of Gradient method (EOG), Sum of

*Corresponding author: ShuzhenWang@mails.cust.edu.cn

Modified Laplacian method (SML), and the Phase Coherence method (PC), etc[11-14]. Scholars such as Huang[15]have used a lot of experiments to prove that SML is in the application of multi-focus image fusion is better than other commonly used sharpness focusing evaluation functions. The SML function is most sensitive to changes in image sharpness under the same conditions, but it takes a long time.

Based on the above research, this paper proposes an improvement to the calculation process of SML, analyzes the time-consuming reason of the algorithm in the calculation process, and optimizes it, thus proposes a fast all-focus image reconstruction technology based on light field imaging, combined with the design according to the fusion rule, the cavity area in the focus area is filled with holes, and error noise is eliminated, and the quality of the fusion image is improved.

2 Principle

2. 1 Calculation of refocused images in different spatial depths

Figure 1 shows the two-plane parametric model of the light field. Let the main lens plane of the light field camera be the (u, v) plane and the sensor plane be the (x, y) plane. The 4D light field recorded by the light field camera is L_F (x, y, u, v) and the integral image of the focal plane of the all-optical camera can be obtained from the classical light radiation formula:

$$I_F(x,y)=\frac{1}{F^2}\sum_{u=1}^{U}\sum_{v=1}^{V}L_F(x,y,u,v) \tag{1}$$

where F is the distance between the main lens plane and the sensor plane, $X \times Y \times U \times V$ represents the *4D* light field matrix L_F *(x, y, u, v)* size. If the distance between the image plane (sensor plane) and the main lens plane is changed from F to F', the new *4D* light field matrix is represented by $L_{F'}(x', y', u', v')$, and at this time, the refocused image at the focal plane of the camera is expressed as

$$I_F(x',y')=\frac{1}{F'^2}\sum_{u'=1}^{U'}\sum_{v'=1}^{V'}L_F(x',y',u',v') \tag{2}$$

Let $F'=\alpha_n F$, where α_n is the focusing coefficient. According to the principle of similar triangles, the coordinates of the new light field and the original light field satisfy:

$$I_{a_nF}(x,y)=\frac{1}{a_n^2F^2}\sum_{u=1}^{U}\sum_{v=1}^{V}L_F([x,y,u,v]\bullet B_{a_n}^T) \tag{3}$$

where B_{a_n} is the coordinate transformation matrix, and the specific form is

$$B_{a_n}=\begin{bmatrix} a_n & 0 & 1-a_n & 0 \\ 0 & a_n & 0 & 1-a_n \\ 0 & 0 & 1 & 0 \\ 0 & 0 & 0 & 1 \end{bmatrix} \tag{4}$$

By changing the value of α_n, the position of the image plane can be changed, and then get refocused images with different spatial depths.

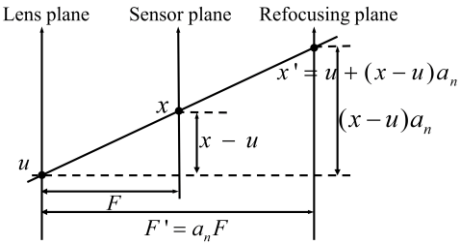

Fig. 1. Digital refocusing principle of light field camera.

2. 2 The improved fast NSML image fusion algorithm

SML reflects the edge feature information of the image, and to some extent, it can properly reflect the focusing characteristics and sharpness of the image. The traditional SML algorithm only calculates the variable step Laplace operator value *ML* for each pixel point in the horizontal and vertical directions, with a single direction and lack of detection on the primary and secondary diagonals, while the NSML algorithm calculates the variable step Laplace operator value for each pixel point in a total of eight directions, horizontal, vertical and diagonal, with the addition of four directions on the diagonal, which are defined as follows.

$$\begin{aligned} ML(x,y) = &\left|2f(x,y) - f(x-step,y) - f(x+step,y)\right| + \\ &\left|2f(x,y) - f(x,y-step) - f(x,y+step)\right| + \left|2f(x,y) - f(x-step,y-step) - f(x+step,y+step)\right| \\ &+ \left|2f(x,y) - f(x+step,y-step) - f(x-step,y+step)\right| \end{aligned} \tag{5}$$

$$\begin{cases} NML(x,y) = \sum_{i=X-N}^{X+N} \sum_{j=Y-N}^{Y+N} \dfrac{ML(i,j)}{1+\sqrt{(i-x)^2+(j-y)^2}} & for\ NML(x,y) \geq T \\ NSML(x,y) = \sum_{i=X-N}^{X+N} \sum_{j=Y-N}^{Y+N} NML(i,j) \end{cases} \tag{6}$$

The *step* is a step change parameter usually taken as 1. The parameter setting is mainly selected according to the noise size, with a small *step* mainly applied to images with less noise interference and a larger *step* mainly applied to images with large noise and brightness changes. Using spatial geometric distance to assign weights, the closer the pixel area to the central pixel point is considered to be more influential, and the weighted approach also suppresses the generation of some noise gradients to a certain extent, while the size of the window *N* value can be reasonably adjusted to expand the detection range, and the selection of a suitable threshold *T* can effectively extract the focused target area.

Multi-focus image fusion using NSML algorithm gives excellent results, but the process is time-consuming, so this paper proposes a fast NSML image fusion algorithm. Set *MI* (*x*, *y*) to be the integral image corresponding to the image at the coordinate point (*x*, *y*), then *MI* (*x*, *y*) is expressed as

$$MI(x,y) = \sum_{i=0}^{x} \sum_{j=0}^{y} MI(i,j) \tag{7}$$

As shown in Figure 2, let the size of NSML accumulation window be $(2N + 1) \times (2N + 1)$, and the four points of *I* (x, y) top-left, top-right, bottom-left and bottom-right are A, B, C and D respectively. Then the *MI* values of points A, B, C and D can be obtained from

Equation (5), respectively. From equations (5), (6) and (7), the NSML of I (x, y) can be calculated as follows.

$$NSML\,I(x,y)=\sum_{i=x-N}^{x+N}\sum_{j=y-N}^{y+N}NML\,I(i,j)=MI_D(x,y)+MI_A(x,y)-MI_B(x,y)-MI_C(x,y) \tag{8}$$

Using a similar approach to that described above, fast *MI* calculations can be achieved, as shown in Figure 3. The *MI* value of D (x, y) can be obtained using Equation (5).

$$MI_D(x,y)=\sum_{i=0}^{x}\sum_{j=0}^{y}NML(i,j)=MI_B(x,y)+MI_C(x,y)-MI_A(x,y)+NML(x,y) \tag{9}$$

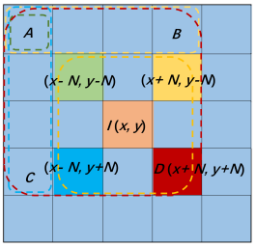

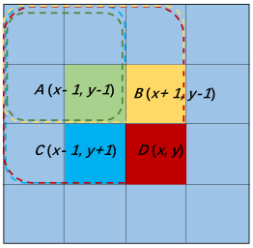

Fig. 2. *I*, *A*, *B*, *C*, *D* position relationship. **Fig. 3.** Fast *MI* calculation schematic.

As can be seen from Equation (9), when calculating *MI* in the direction of pixel points from top to bottom and left to right, since the *MI* values of neighboring pixel points *A*, *B*, and *C* have already been calculated, the *MI* value of point *D* can be calculated directly and quickly from the *MI* values of points *A*, *B*, and *C*, eliminating the accumulation process of Equation (7). Compared with the unimproved NSML computation process, the time consumed by the fast NSML computation process does not vary with the accumulation window parameter *N*, which greatly improves the efficiency of the NSML fusion algorithm.

2. 3 Integration rules

In this paper, the initial decision image I (x, y) is obtained by selecting the focus region for the focus stack image using the larger NSML value. For the possible existence of noise and isolated points in the decision image, median filtering is used to remove some isolated points in the initial decision map to reduce the impact of noise, and the edges of the detected focus region are smoothed by mean filtering, and then the voids are filled using the following equation.

$$\begin{aligned} AvgF(x,y)&=\frac{I_{a1}(x,y)+I_{a2}(x,y)+\ldots+I_{an}(x,y)}{n}\\ DiffF(x,y)&=I(x,y)-AvgF(x,y)\end{aligned} \tag{10}$$

The mean image difference represents the difference between the primary decision map and the mean image, and the final image fusion is performed by combining the focal stack images, and the final fusion rule is given in the following equation.

$$F(x,y)=\begin{cases}I(x,y), DiffF(x,y)\geq 0\\ \max I_{an}(x,y), DiffF(x,y)<0\end{cases} \tag{11}$$

where F (x, y) is the final fused image, $max\ I_{an}$ (x, y) is the pixel grayscale value of the pixel

point at the focal stack image sequence.

3 Experiment and analysis

In order to verify the effectiveness of the algorithm in this paper, the experiments were conducted using the original images taken by Lytro optical field camera (experimental test data from Lytro first generation dataset). Figure 4 shows the acquired light field image and its local enlargements to further show the detailed information of the images. The light field refocusing of the image in Figure 4 can reconstruct a series of images corresponding to different focal planes, i.e., a multi-focused image source set, as shown in Figure 5. Figure 6 shows two refocused images with different spatial depths calculated according to Equation (3). The depth of focus gradually changes from foreground to background.

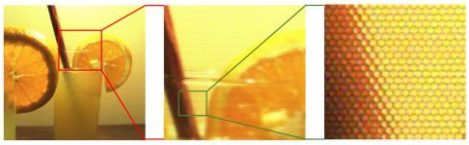

Fig. 4. The acquired light field image

Fig. 5. Multi focus image source set based on light field image.

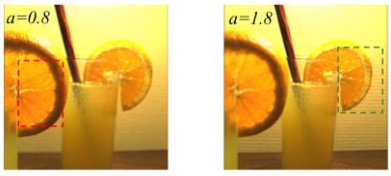

Fig. 6. Two refocused images with different spatial depths.

As shown in Figure 7, the traditional SML algorithm, the DCT algorithm and the fast NSML algorithm proposed in this paper were used to fuse two different depths of the focal images for multi-focus image fusion. The mutual information (QMI), standard deviation (STD) and information entropy (QEN) method were used to calculate the sharpness of the fusion result maps of different methods, and the calculation results are shown in Table 1. The larger the values of QMI, STD and QEN, the better the visual information of the image.

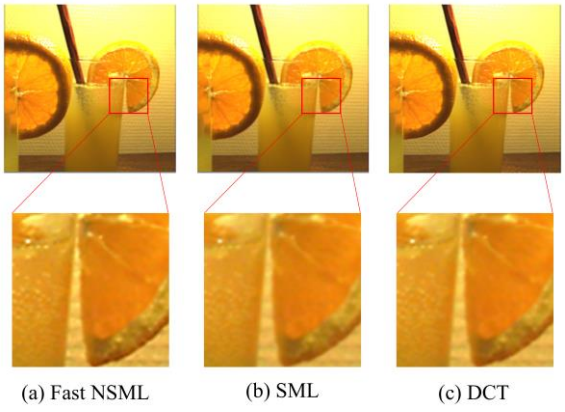

Fig. 7. Multi focus image fusion using different methods.

The visual comparison of the images and the fusion quality evaluation results show that the fused images obtained by using the proposed fast NSML algorithm for multi-focus

image fusion are better than the SML and DCT algorithms in terms of QMI, STD and QEN, and the fused images are rich in information. In terms of time consumption, compared with the conventional NSML algorithm and tested using the same parameters (N=30, $step$=1), the results obtained are shown in Table 2.

Table 1. Image objective evaluation results.

Evaluation Indicators	SML	DCT	Fast NSML
QMI	1.478	1.399	1.659
STD	3.231	3.186	3.485
QEN	7.319	7.054	7.541

Table 2. Comparison of processing time of fusion algorithms.

Fusion Algorithm	Processing time(s)
Conventional NSML	31.169
Fast NSML	2.968

As can be seen from the table, the fast NSML fusion algorithm has a significant reduction in algorithm processing time compared to the traditional NSML algorithm. The traditional NSML algorithm takes 31.169 s, while the fast NSML algorithm takes 2.968 s. The real-time performance is improved by about 10 times. As a result, the fast NSML algorithm achieves excellent fusion results with better performance in real-time.

4 Conclusions

In this paper, we use optical field refocusing to obtain a multi-focus image source set, and then use the fast NSML algorithm to fuse the images to obtain high-quality full-focus images. It is demonstrated that this method can reconstruct the full-focus images with better results than the traditional SML and DCT full-focus fusion methods, and effectively reduce the processing time of image fusion while achieving excellent fusion results.

References

1. N. Ren, et al. Stanford University Cstr (2005).
2. N. Ren, ACM T GRAPHIC,**24**(2005).
3. X. Liu, et al. *3D Image Acquisition and Display: Technology, Perception and Applications* (2018).
4. W. Chantara, M. Jeon. APPS, **9**(2019).
5. J.G. Liu, INT J REMOTE SENS, **21**(2010).
6. S. Li, X. Kang and J. Hu, IEEE Trans Image Process, **22**(2013).
7. C. Feichtenhofer, H. Fassold and P. Schallauer. IEEE SIGNAL PROC LET, **20**(2013).
8. X. Qin, et al., INFRARED PHYS TECHN, **85**(2017).
9. F. Fakhari, M.R. Mosavi and M.M. Lajvardi, IET IMAGE PROCESS, **11**(2017).
10. T. Stathaki, *Image Fusion: Algorithms and Applications* (2008).
11. S.K. Nayar, Y. Nakagawa, IEEE T PATTERN ANAL, **16**(1994).
12. Z. Hu, et al., APPL INTELL, **51**(2021).
13. M. Hossny, S. Nahavandi and D. Creighton, ELECTRON LETT, **44**(2008).
14. T.G. Stanciu, M. Drgulinescu and G.A. Stanciu, U POLITEH BUCH SER A, **73**(2011).
15. Z. Jing, et al., Springer International Publishing (2018).